



This is a repository copy of *Freeze-thaw resistance of steel fibre reinforced rubberised concrete*.

White Rose Research Online URL for this paper:
<http://eprints.whiterose.ac.uk/142311/>

Version: Accepted Version

Article:

Alsaif, A. orcid.org/0000-0002-3057-0720, Bernal, S.A. orcid.org/0000-0002-9647-3106, Guadagnini, M. orcid.org/0000-0003-2551-2187 et al. (1 more author) (2019) Freeze-thaw resistance of steel fibre reinforced rubberised concrete. *Construction and Building Materials*, 195. pp. 450-458. ISSN 0950-0618

<https://doi.org/10.1016/j.conbuildmat.2018.11.103>

Article available under the terms of the CC-BY-NC-ND licence
(<https://creativecommons.org/licenses/by-nc-nd/4.0/>).

Reuse

This article is distributed under the terms of the Creative Commons Attribution-NonCommercial-NoDerivs (CC BY-NC-ND) licence. This licence only allows you to download this work and share it with others as long as you credit the authors, but you can't change the article in any way or use it commercially. More information and the full terms of the licence here: <https://creativecommons.org/licenses/>

Takedown

If you consider content in White Rose Research Online to be in breach of UK law, please notify us by emailing eprints@whiterose.ac.uk including the URL of the record and the reason for the withdrawal request.



eprints@whiterose.ac.uk
<https://eprints.whiterose.ac.uk/>

Freeze-Thaw Resistance of Steel Fibre Reinforced Rubberised Concrete

Abdulaziz Alsaif^{a,b*}, Susan A. Bernal^{c,d}, Maurizio Guadagnini^a
Kypros Pilakoutas^a

^aDepartment of Civil and Structural Engineering, The University of Sheffield, Sir Frederick Mappin Building, Mappin Street, Sheffield, S1 3JD, UK.

^bDepartment of Civil Engineering, King Saud University, P. O. Box 800, Riyadh 11421, Saudi Arabia.

^cDepartment of Materials Science and Engineering, The University of Sheffield, Sir Robert Hadfield Building, Mappin Street, Sheffield, S1 3JD, UK

^dSchool of Civil Engineering, University of Leeds, Woodhouse Lane, Leeds, LS2 9JT, UK

* Corresponding author: email: asaalsai@sheffield.ac.uk; Tel: +44 (0) 114 222 5729,
Fax: +44 (0) 114 2225700

Abstract

This study evaluates the freeze-thaw performance of steel fibre reinforced rubberised concretes (SFRRuC) engineered for flexible concrete pavements. The effect of large volumes of fine and coarse rubber particles (i.e. 30% and 60% volumetric replacement of natural aggregates) is determined for concretes reinforced with 40 kg/m³ of a blend of manufactured steel fibres and recycled tyre steel fibres. The freeze-thaw performance is assessed through surface scaling, internal damage, residual compressive strength and flexural behaviour. The results show that SFRRuC are able to withstand 56 freeze-thaw cycles with acceptable scaling and without presenting internal damage or degradation in mechanical performance. This indicates that SFRRuC can perform well under extreme freeze-thaw conditions and can be used to construct long-lasting flexible pavements as a sustainable alternative to asphalt concretes.

Keywords: Freeze-thaw; Frost resistance; Rubberised concrete; Steel fibre concrete; Flexible pavements.

33 1 Introduction

34

35 The use of concrete pavement slabs in regions experiencing severe freeze-thaw cycles is
36 challenging, as concretes used for this application must withstand harsh environmental
37 conditions during their service-life. One of the main factors compromising the durability of
38 concrete pavements in such conditions is that drastic changes in temperature produce extra
39 internal stresses causing concrete deterioration [1, 2]. Ice lenses can also form beneath the
40 concrete surface as a result of uneven frost action on the subgrade and can potentially create
41 unsupported regions in the pavement structure and cause additional flexural stresses [3].
42 Furthermore, de-icing salts, which are used to melt ice and snow, contain high volumes of
43 sodium and/or magnesium chloride and can induce corrosion of the steel reinforcement and
44 surface spalling [4, 5]. Hence, it is required to design concretes that can meet the mechanical
45 strength requirements for paving, with the ability to withstand aggressive in-service conditions
46 such as chlorides attack and freeze-thaw.

47

48 According to the European Tyre Recycling Association (ETRA) [6], each year in the 28
49 European member states and Norway around 300 million post-consumer tyres are discarded as
50 waste. Much of these end up in landfills or are incinerated, despite the fact that they contain
51 high performance constituent materials. According to ETRA [6], the composition of car tyres
52 on the European Union market (by weight) are 48% rubber, 22% carbon black, 15% metal, 5%
53 textile, and 10% others. Strict environmental protocols have been considered in most developed
54 countries to control the disposal of waste tyres and the European Directive 1991/31/EC [7] has
55 forbidden the land filling of whole post-consumer tyres since 2003 and shredded tyres since
56 2006 [8-10]. The European Directive 2008/98/EC [11] has provided a disposal hierarchy to
57 encourage the management of post-consumer tyres that places reuse and recycling above
58 incineration. A possible waste management solution is to find use for the post-consumer tyre
59 materials in the construction industry. This improves sustainability by preventing
60 environmental pollution as well as saving natural aggregate from depletion, and it is
61 economically viable as some of the costly conventional materials (e.g. steel fibres) can be
62 saved.

63

64 During the last three decades, rubber aggregates have been used in asphalt-rubber mixtures for
65 pavement applications [12]. It has been noted that the use of rubber helps to reduce noise and
66 increase resistance to temperature variation and freeze-thaw action, thus lowering maintenance
67 costs and enhancing service life [13, 14]. The use of rubber aggregates as a partial substitution
68 of natural aggregates in concrete has also been investigated by several researchers [8, 15-17].
69 It has been demonstrated that, compared to conventional concrete, rubberised concrete (RuC)
70 has larger deformability [15, 18], lower density [19-21], and higher sound absorption, skid and
71 impact resistance as well as enhanced electrical and thermal insulation [10, 22-24]. Conversely,
72 RuC suffers from increased air content as well as reduced workability, strength and stiffness
73 [8, 25, 26]. As a result, RuC is rarely used in structural applications.

74

75 The durability properties of RuC are also not well understood. Few studies have assessed the
76 freeze-thaw resistance of RuC and most focused on the resistance of RuC containing crumb
77 rubber only [1, 2, 27-30]. Savas et al. [30] investigated the freeze-thaw resistance of RuC
78 containing different amounts of crumb rubber. They observed that RuC mixes with replacement
79 ratios of 10% and 15% by weight of cement (2–6 mm in size) exhibited durability factors (DFs)
80 higher than the minimum 60% after 300 freeze-thaw cycles specified by ASTM C666/C666M-
81 15 [31], whereas mixes with 20% and 30% could not meet the minimum DF recommended.
82 Similarly, Kardos and Durham [32] assessed the rapid freeze-thaw resistance of plain concrete
83 and RuC mixes with up to 50% sand replacement by volume. The authors found that RuC
84 containing 10% crumb rubber exhibited the highest DF followed by the 20% RuC while the
85 plain concrete and 30% RuC, showed comparable DFs. The 40% RuC and 50% RuC failed to
86 withstand freeze-thaw action after 300 cycles as their DFs fell below 60%. Richardson et al.
87 [28, 29], on the other hand, indicated that the addition of 0.6% by weight of crumb rubber with
88 size smaller than 0.5 mm provided significant freeze-thaw protection in concrete.

89

90 Deterioration of concrete subjected to repeated freeze-thaw actions occur due to the formation
91 of micro ice bodies within the concrete pores, which expand up to 9% compared to the volume
92 of water [33, 34]. If the concrete paste becomes critically saturated and there is no space for
93 this volume expansion, hydraulic pressures and tensile stresses can be generated in the pores,
94 contributing to pore enlargement [35]. Consequently, the enlarged pores can be filled with
95 water from the environment due to water uptake phenomena, causing larger tensile stress when

96 frozen again and eventually leading to deterioration. Hence, the pore structure governs the rate
97 and level of damage caused by freeze-thaw. More interconnected and larger pores are expected
98 to lead to more water uptake and damage. The freeze-thaw resistance of concrete can be
99 improved by providing air-entraining agents to create empty and closely spaced bubbles, which
100 act as receiver of the excess water, thus relieving the pressure created in the concrete due to ice
101 formation. In full saturation conditions, however, “the hydraulic pressure theory” is not
102 applicable since non-frozen water cannot find a way to escape [36]. It is believed that crumb
103 rubber particles can promote the formation of pores of similar quality to those created by air-
104 entraining agents [28, 37]. Khalo et al. [25] attributed the entrapment of air to the hydrophobic
105 nature and rough surfaces of rubber particles, which entrap air during the mixing process.
106 Hence, it is evident that the amount and size of rubber particles incorporated play a major role
107 in the RuC freeze-thaw resistance, but there appears to be a limit to the replacement ratio that
108 can lead to beneficial results. It has been reported for rubberised mortars and concretes that the
109 amount of rubber replacement should be limited to a maximum of 10% [2] or 30% [32] by
110 volume of fine aggregate in order to obtain acceptable durability.

111

112 In a recent study, the authors [38] demonstrated that the inclusion of fibres in RuC with high
113 volumes of rubber (e.g. 30% or 60%) promote the development of SFRRuC with enhanced
114 flexibility and ductility characteristics and flexural strengths that comply with the
115 specifications defined in pavement design EN 13877-1 [39]. It has also been identified [40]
116 that the substitution of natural aggregate by rubber particles increases the permeability of
117 SFRRuC (i.e. volume of permeable voids and sorptivity) as rubber content increases. However,
118 this increment is minor and the permeability properties of these concretes lie within the range
119 of highly durable concretes. Furthermore, SFRRuC exhibit very high resistance to chloride
120 permeability when assessed under accelerated wet-dry cycles [40]. The combination of such
121 properties makes SFRRuC mixes ideal candidates for flexible concrete pavements. However,
122 the effect of large volume of rubber on freeze-thaw resistance needs to be addressed. Due to
123 the weak bond between cementitious materials and rubber particles [25, 26], micro-cracks
124 forming in RuCs might propagate locally at a fast rate, making these materials more prone to
125 damage. However, the authors hypothesised that this issue would be greatly mitigated by the
126 inclusion of fibres in RuC as fibres tend to bridge micro-cracks and resist their opening. Hence,
127 this study aims to examine the influence of freeze-thaw on the performance of SFRRuC under
128 accelerated conditions. Performance is assessed through visual inspection of the specimens,

129 mass loss, coefficient of thermal expansion (CTE), changes in relative dynamic modulus of
130 elasticity (RDM), and residual mechanical properties including compressive strength, flexural
131 strength, flexural modulus of elasticity and toughness.

132

133 **2 Experimental Programme**

134

135 **2.1 Materials and concrete mix designs**

136 2.1.1 Materials

137

138 Concrete mixtures were produced using a ternary blend of Portland lime cement type CEM II
139 52.5N, with silica fume (SF) and pulverised fuel ash (PFA) as cement replacements (10% by
140 weight for each). Two types of high range water-reducing admixtures were used: a)
141 polycarboxylate polymer plasticiser and b) superplasticiser

142

143 Natural river sand with particle size of 0/5 mm and specific gravity (SG) of 2.64 was used as
144 fine aggregate (FA), while natural river gravel with particle sizes of 5/10 mm and 10/20 mm
145 and a SG of 2.65 was employed as coarse aggregate (CA). Rubber aggregates used in this
146 experimental study were recovered mechanically from post-consumer tyres. The fine rubber
147 (FR) particles were supplied in three different sizes, 0/0.5 mm, 0.5/2 mm and 2/6 mm, and
148 were used to replace 22.2%, 33.4%, 44.4% of FA volume, respectively. The course rubber
149 (CR) particles were provided in two sizes, 5/10 mm and 10/20 mm, and were used to replace
150 the CA in equal amounts. The specific gravity of 0.8, determined by the authors [38], was
151 employed to calculate the volume of rubber particles. Fig. 1 shows the particle size distribution
152 of all aggregates used in this study, obtained according to ASTM-C136 [41].

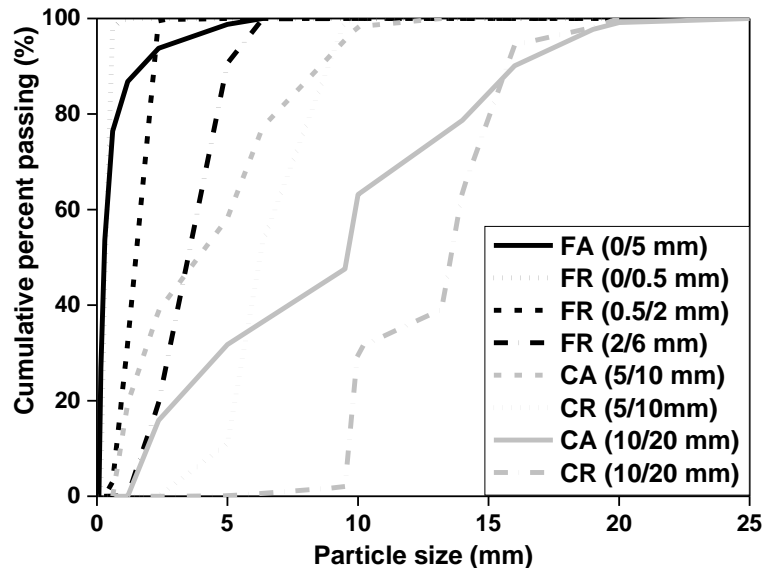


Fig. 1 Particle size distributions

153

154

155

156 2.1.2 Concrete mix designs

157

158 Four different concrete mixes were prepared in this study including a plain concrete mix, a
 159 steel fibre reinforced concrete (SFRC) mix, and two SFRC rubberised concrete (SFRRuC)
 160 mixes, in which rubber aggregates were used as partial replacement for both FA and CA with
 161 30% or 60% by volume. The amount of steel fibres added in the SFRC and SFRRuC mixes
 162 was 40 kg/m^3 , as used in structural concrete, using equal amount of: a) crimped type
 163 manufactured steel fibres (MSF) with lengths of 55 mm and diameters of 0.8, and b) recycled
 164 tyre steel fibres (RTSF) with lengths between 15-45 mm (>60% by mass) and diameters <0.3
 165 mm. Further details about the fibres characteristics are reported in [38, 42].

166

167 A mix ID was adopted for easy reference. It contains a number and a letter, where the number
 168 can be 0, 30 or 60, denoting the volumetric percentages of rubber aggregates used as partial
 169 replacement of natural aggregates, while the letter can be either P or BF (Plain or Blend of
 170 Fibres, respectively), referring to the absence or presence of the steel fibre reinforcement in the
 171 concrete mix. Table 1 shows the mixes IDs and variables.

172

173

Table 1 Mixes IDs and variables

| Mix ID | OP | 0BF | 30BF | 60BF |
|-------------------------------------|----|-----|------|------|
| FR replacing FA by volume (%) | 0 | 0 | 30 | 60 |
| CR replacing CA by volume (%) | 0 | 0 | 30 | 60 |
| Amount of MSF (kg/m ³) | 0 | 20 | 20 | 20 |
| Amount of RTSF (kg/m ³) | 0 | 20 | 20 | 20 |

175

176 All concretes assessed in this study were designed with 340 kg/m³ of Portland cement, 42.5
 177 kg/m³ of SF, 42.5 kg/m³ of PFA , 820 kg/m³ of FA, 1001 kg/m³ of CA, 150 l/m³ of tap water
 178 (water /cement = 0.35), with 2.5 l/m³ of plasticiser and 5.1 l/m³ of superplasticiser. All mix
 179 design parameters were kept constant in this study except from the aggregates volume (see
 180 section 2.1.1). This study targeted slump of class S3 according to EN 206 [43] or higher (≥ 90
 181 mm), therefore, the amount of plasticiser was also increased to 3.25 l/m³ for 30BF mix and to
 182 4.25 l/m³ for 60BF mix to attain the targeted slump. The adopted concrete mix design was
 183 selected based on the outcomes of a previous study [21] evaluating RuC, in which it was
 184 identified that similar large volumes of aggregate replacements do not induce excessive
 185 degradation in fresh properties compared with reference concretes without rubber.

186

187 2.1.3 Mixing, casting and curing procedure

188

189 The production of the concrete mixes started with dry mixing natural and rubber aggregates for
 190 30 s using a pan mixer. Half of the total amount of water was then introduced to the mixer,
 191 and the materials were mixed for another 1 min. Subsequently, mixing was halted for 3 min, to
 192 allow aggregates to gain saturation, and the cementitious materials were added. After that,
 193 mixing was continued for 3 min during which the remaining water and chemical admixtures
 194 were gradually added. Finally, the steel fibres were manually integrated, and mixing was
 195 continued for another 3 min.

196 Prior to casting, the concrete fresh properties including slump, air content and unit weight were
 197 assessed based on methods described in EN 12350-2 [44], EN 12350-7 [45], and EN 12350-6
 198 [46], respectively. Table 2 summarises the fresh properties of the concrete mixes. The results
 199 show that the inclusion of rubber particles in the fresh concrete mixes reduces the slump and
 200 unit weight, and increases the air content.

201

Table 2 Fresh properties of the tested concrete mixes

| Mix ID | 0P | 0BF | 30BF | 60BF |
|----------------------------------|------|------|------|------|
| Slump (mm) | 235 | 200 | 155 | 110 |
| Air content (%) | 1.7 | 1.3 | 2.3 | 2.9 |
| Unit weight (kg/m ³) | 2401 | 2425 | 2175 | 1865 |

202

203 Concrete was cast in the moulds using two layers of casting (according to EN 12390-2) [47]
204 and was vibrated on a shaking table (25s per layer). The specimens were then cured in the
205 moulds for 48 h with wet hessian and sealed with plastic. Subsequently, all specimens were
206 stored in a mist room at a temperature of 21 °C ± 2 and relative humidity of 95 ± 5% for 10
207 months. This curing age was selected considering that in countries experiencing severe winters,
208 concrete casting on-site typically takes place in spring (or summer) and therefore it is most
209 likely that the first freeze-thaw will be experienced within 10 months of age.

210

211 Four cubes and three prisms per mix were removed from the mist room, marked as ‘F-T’ and
212 subjected to freeze-thaw conditions, while a similar number of specimens was kept as ‘control’
213 in the mist room. The compressive strength and flexural behaviour of all ‘F-T’ and ‘control’
214 specimens were evaluated at the end of the freeze-thaw conditioning period. Two prisms per
215 mix were used to assess the coefficient of thermal expansion (CTE) as described in section 3.2.

216

217 **2.2 Test set-up and instrumentation**

218

219 **2.2.1 Freeze-thaw testing**

220

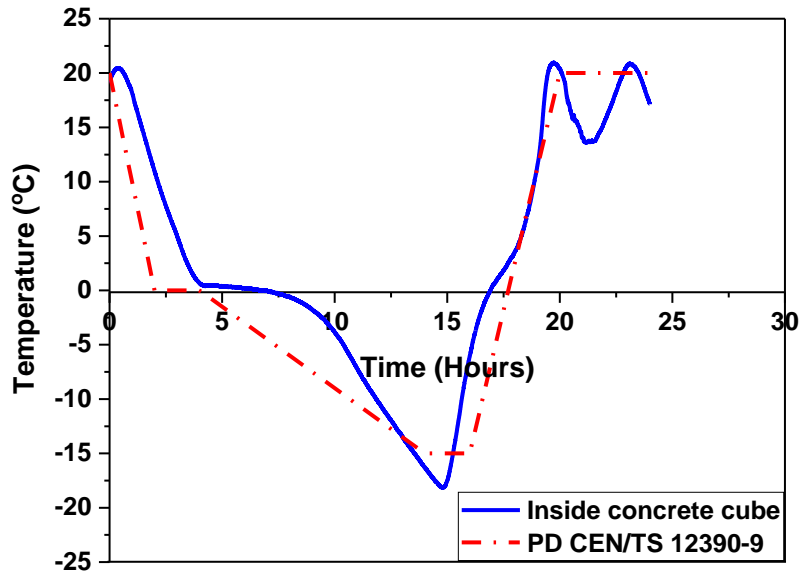
221 The freeze-thaw resistance of concrete cubes and prisms was assessed based on: (i) visual
222 analysis in terms of damage caused by freeze-thaw action, (ii) mass loss due to cubes scaling
223 following the recommendation of PD CEN/TS 12390-9 [48], (iii) beam tests according to PD
224 CEN/TR15177 [49] to assess the internal damage of concrete prisms through the evaluation of
225 their RDMs using the measurements obtained from ultrasonic pulse transit time (UPTT), and
226 (iv) residual compressive strength and flexural behaviour.

227

228 The concrete specimens were placed in stainless steel containers and were fully immersed in a
229 3% NaCl solution. The containers were then placed into a chamber that was programmed to

230 apply continuous cycles of freeze and thaw with temperature ranging from -15 °C to 20 °C and
 231 controlled through a thermocouple embedded in the centre of a concrete cube. Fig. 2 shows
 232 the experimental temperature profile compared with the desired temperature profile specified
 233 in PD CEN/TS 12390-9 [48].

234



235

236 **Fig. 2** Temperature profile measured in the centre of a concrete cube using a thermocouple,
 237 compared with that of PD CEN/TS 12390-9 [48]

238

239 The mass loss and UPTT were determined after 7, 14, 28, 42 and 56 freeze-thaw cycles. At
 240 each of these defined cycles, during the thawing phase, the concrete cubes and prisms were
 241 removed and first visually examined in terms of surface damage. The cubes were then
 242 thoroughly brushed to remove any loose parts and then weighed. All detached materials were
 243 collected, oven dried for 24 hours at 105 °C and weighed to the nearest 0.1g. The percentage
 244 of cumulative mass loss after n cycles, was calculated according to Equation (1):

245

$$246 \text{ Cumulative mass loss (\%), } n = \frac{\sum_{i=1}^n M_{d,i}}{M_0} \cdot 100 \quad (1)$$

247

248 where, $M_{d,n}$ is the mass of the oven dried scaled material collected after cycle n, and M_0 is the
 249 initial mass of specimens after curing and before testing.

250

251 Similarly, the concrete prisms were thoroughly brushed, surface dried, and were then fitted
 252 with two transducers on the two opposite sides of the prisms to measure the UPTT. The

253 transducers were pressed against the concrete surfaces, using the same pressure each time, until
254 a constant minimum value was achieved. The RDM of elasticity after n cycles, was calculated
255 using Equation (2) below;

$$257 \quad \text{RDM, n (\%)} = \left(\frac{\text{UPTT}_0}{\text{UPTT}_n} \right)^2 \cdot 100 \quad (2)$$

258
259 where UPTT_0 is the initial UPTT of the specimen, in μs , while UPTT_n is the specimen UPTT
260 after n freeze-thaw cycles, in μs . Cubes and prisms were then returned to the containers with
261 fresh 3% NaCl solution and test was resumed.

263 2.2.2 Compressive cube tests and flexural tests on prisms

264
265 Concrete cubes were tested under uniaxial compressive loading according to EN 12390-3 [50]
266 at a loading rate of 0.4 MPa/s. Concrete prisms were tested under 4-point bending test
267 configuration following the recommendations of the JSCE [51], using an electromechanical
268 testing machine. The net mid-span deflection was recorded by two linear variable differential
269 transformers (LVDTs), placed on an aluminium yoke. The load was applied in displacement
270 control at a constant rate of deflection at the mid-span of the prism of 0.2 mm/min until a
271 deflection of 6 mm.

273 2.2.3 Coefficient of thermal expansion

274
275 The CTE was determined according to the TI-B 101 procedure [52] using two duplicate prisms
276 per mix. The CTE of the rubber particles used in this study was also determined to be
277 approximately $80 \times 10^{-6} \text{ m/mK}$, which is 10 times higher than that of the limestone natural
278 aggregates used in this study, and obtained from FDA [53]. Such significant difference in CTE
279 may induce internal stresses during the freeze-thaw cycles.

280

281

282

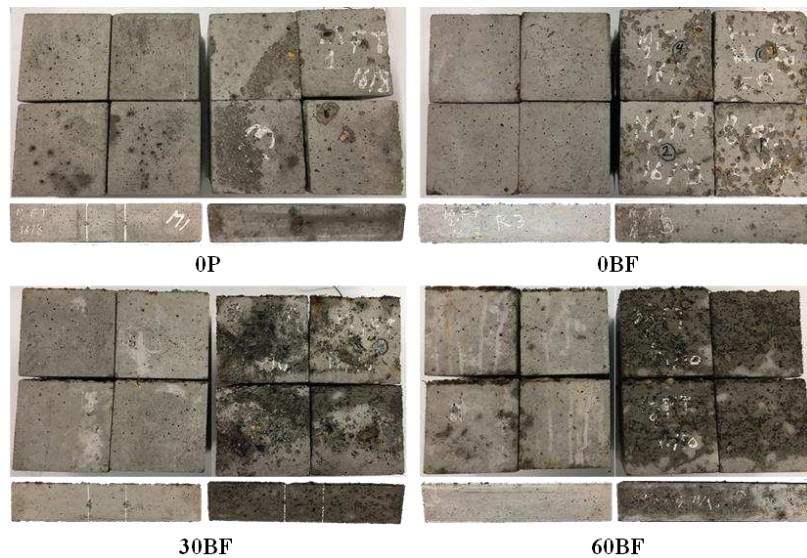
283 **3 Results and Discussion**

284

285 **3.1 Visual inspection**

286

287 Fig. 3 shows the appearance of the tested specimens before and after completing 56 cycles of
288 freeze-thaw action. Surface scaling and concrete pop-outs are the two signs of deterioration
289 that are observed in all tested specimens. Surface scaling (i.e. delamination) is expected to
290 develop when internal stresses exceed the tensile or shear strength of the surface layer, whilst
291 the build-up of pressure around the coarse aggregate particles can cause the concrete between
292 the particles and the nearest concrete face to pop-outs [54].



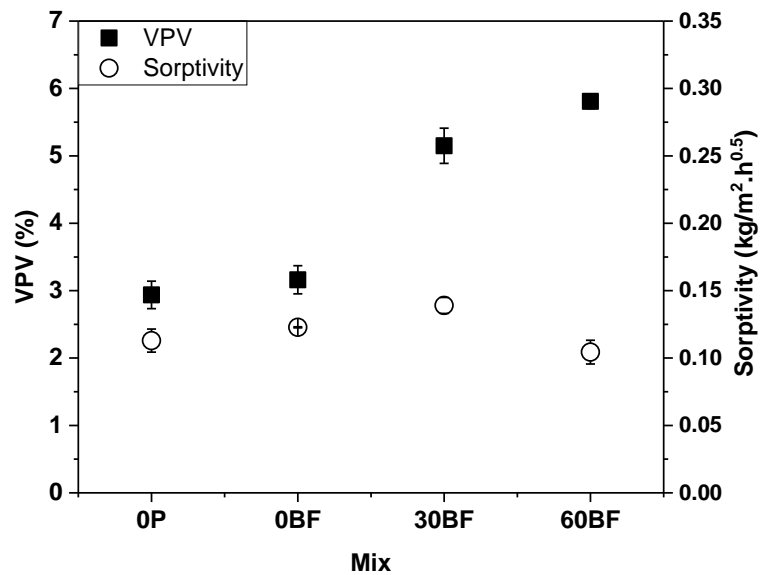
293

294 **Fig. 3** Specimens appearance before (left) and after (right) completing 56 cycles of freeze-
295 thaw action

296

297 ASTM C672/C672M – 12 [55] specifies a visual rating category depending on the severity of
298 surface scaling, as shown in Table 3. Based on the appearance of the concretes after exposure
299 (Fig. 3), concretes without rubber aggregates (i.e. 0P and 0BF) are rated 3, while SFRRuC
300 specimens (i.e. 30BF and 60BF) are rated 4. The amount of concrete scaling and mortar coming
301 off at the end of the freeze-thaw cycles is higher in rubberised concrete. This is a likely
302 consequence of the higher volume of permeable voids (VPV) identified in SFRRuC (see Fig.
303 4 [40]), and the resulting increase in water uptake of the samples during testing compared to
304 specimens without rubber aggregates. It has been reported [56] that the connectivity of pores
305 is higher at the surface of the concrete specimens and typically increases at higher freeze-thaw

306 cycles. Therefore, concretes with higher permeability are expected to suffer more severe
 307 damage. Despite the fact that the SFRRuC specimens show moderate to severe scaling, they
 308 withstood 56 freeze-thaw cycles without severe damage.



309
 310 **Fig. 4** VPV (left) and sorptivity (right) of all tested concretes [40]

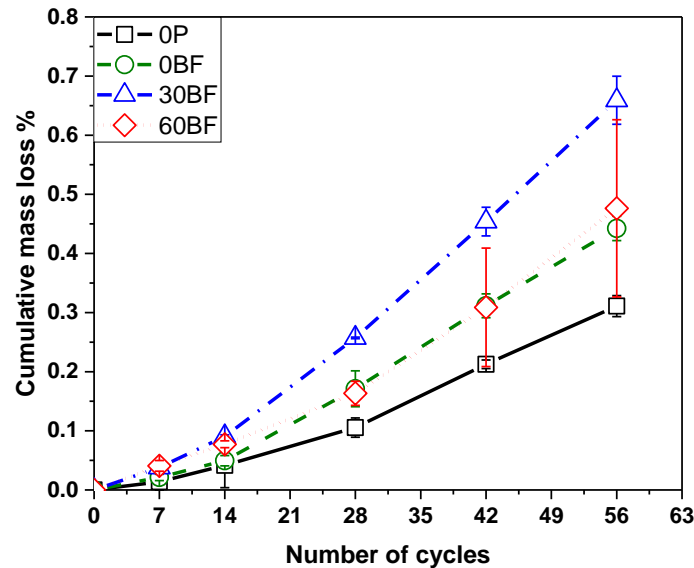
311
 312 **Table 3** Surface scaling rating adapted from ASTM C672/C672M – 12 [55]

| Rating | Condition of surface |
|--------|--|
| 0 | No scaling |
| 1 | Very slight scaling (3 mm [1/8 in.] depth max., no coarse aggregate visible) |
| 2 | Slight to moderate scaling |
| 3 | Moderate scaling (some coarse aggregate visible) |
| 4 | Moderate to severe scaling |
| 5 | Sever scaling (coarse aggregate visible over entire surface) |

313
 314 **3.2 Mass of scaled concretes**

315
 316 Fig. 5 shows the mean cumulative mass loss versus the number of freeze-thaw cycles. Error
 317 bars represent one standard deviation of four measurements. It is evident that OP specimens
 318 exhibit minimal mass loss throughout the test, while OBF and 60BF specimens show similar
 319 mass loss behaviour, which is higher than OP. The SFRRuC specimens with 30% rubber
 320 replacement, 30BF, display the highest rate of mass loss, especially after 14 freeze-thaw cycles.
 321 A previous study by the authors [40] on the transport properties of the same four concrete mixes

322 shows that 30BF specimens present the highest sorptivity values (see Fig. 4). The higher
 323 sorptivity for the 30BF specimens was attributed to the large amount of fine pores which
 324 facilitated water uptake and caused these specimens to be more prone to damage due to freeze-
 325 thaw cycles. On the other hand, owing to the high amount of large coarse rubber particles and
 326 the non-sorptive nature of rubber, a reduction in sorptivity was observed in the 60BF
 327 specimens.



328
 329 **Fig. 5** Cumulative mass loss as a function of freeze-thaw cycles

330
 331 For all concrete mixes, the ratios between the masses of scaled materials after completing 56
 332 freeze-thaw cycles (M_{56}) to that after 28 cycles (M_{28}) are lower than two, and the M_{56} are less
 333 than 1.0 kg/m^2 (see Table 4). Hence, they all fall under the acceptable resistance category, as
 334 specified by the Swedish standard SS 13 72 44 ED [57]. Consequently, this study contradicts
 335 previous work [2, 32] and shows that when using fibres, the amount of rubber aggregates can
 336 be significantly increased (up to 60%) without compromising durability.

337
 338 The high resistance to freeze-thaw exhibited by the tested concretes can not be attributed to
 339 differences in thermal properties as minimal changes in the coefficient of thermal expansion
 340 (CTE) were obtained (see Table 5). This indicates that rubber aggregates may counteract the
 341 freeze-thaw effect even in highly porous concretes due to their low stiffness, which offers less
 342 resistance to expansion. It should also be noted that the addition of rubber increases air
 343 entrainment (see VPV in Fig. 4), as found in [40], which can also create a pressure release

344 system for freeze-thaw phenomena [58]. Furthermore, rubber particles, with their excellent
 345 damping characteristic [20, 59], may contribute somehow in balancing the internal stresses and
 346 act like absorbers for the temperature and freeze-thaw induced stresses and deformations [4].
 347 The fibre blends also participate by bridging and controlling cracks.

348

349 **Table 4** Mass loss results for all concrete mixes

| Mix | M_{56}/M_{28} | Mass of scaled materials after 56 cycles, M_{56} (kg/m ²) |
|------|-----------------|---|
| 0P | 1.5 | 0.5 |
| 0BF | 1.1 | 0.6 |
| 30BF | 1.2 | 0.9 |
| 60BF | 1.9 | 0.7 |

350

351 **Table 5** Coefficient of thermal expansions obtained for all concrete mixes

| Mix | Coefficient of thermal expansion $\times 10^{-6}$ m/mk |
|------|--|
| 0P | 10.3-12.2 |
| 0BF | 10.3-11 |
| 30BF | 9.0-11.6 |
| 60BF | 9.7-12.9 |

356

357 **3.3 Effect of freeze-thaw on mechanical performance**

358

359 **3.3.1 Compressive strength**

360

361 Table 6 summarises the average compressive strength and standard deviation (in brackets)
 362 derived from testing four specimens for each of the examined concretes. As expected, the
 363 addition of blended fibres enhances the compressive strength of control specimen 0BF by 7%
 364 with respect to 0P. The partial replacement of natural aggregates with rubber particles,
 365 however, considerably reduces the compressive strength reporting an average reduction of 58%
 366 for 30BF and 88% for 60BF compared to 0BF. The two mechanisms responsible for such
 367 degradation in compressive strength are: (i) the lower stiffness and higher Poisson ratio of
 368 rubber compared to natural aggregates, and (ii) bond defects between rubber particles and

369 matrix [25, 26]. Further discussions regarding the compressive strength reduction mechanism
370 in SFRRuC are reported in [38], where similar results were obtained.

371

372 **Table 6** Average compressive strength results of all concrete mixes

| Mix | Compressive strength (MPa) | | |
|------|----------------------------|-----------|-----------------------|
| | Control | F-T | Change on control (%) |
| 0P | 111 (3.8) | 108 (3.8) | -3 |
| 0BF | 118 (0.9) | 110 (7.7) | -7 |
| 30BF | 50 (4.0) | 40 (5.3) | -20 |
| 60BF | 14 (3.0) | 12 (2.0) | -14 |

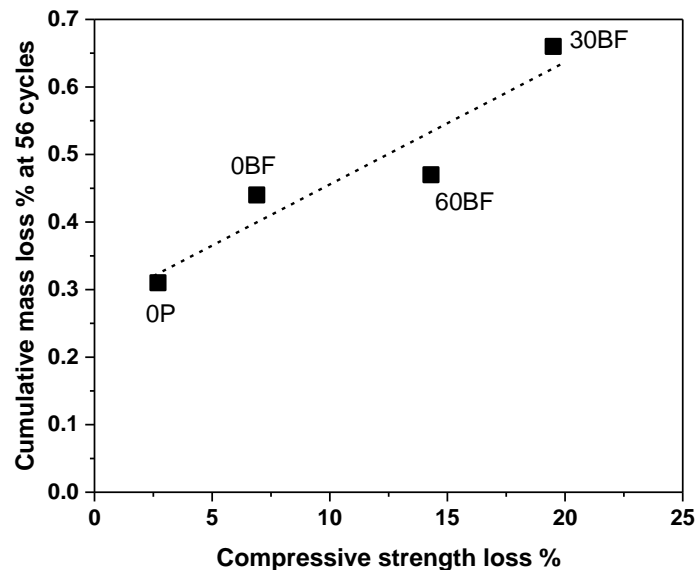
373

374 After 56 cycles of freeze-thaw (F-T), all concrete specimens exhibit minor compressive
375 strength loss compared to the control specimens of the same mixes. The slight reduction in the
376 compressive strength indicates that the freeze-thaw action has affected mostly the surface of
377 the concrete, without compromising its internal integrity.

378

379 A good correlation is identified between the compressive strength and cumulative mass loss
380 for all concrete specimens at the end of the 56 cycles (see Fig. 6). The 30BF specimens show
381 the highest amount of cumulative mass loss, 0.66%, and compressive strength loss, 20%, which
382 were most likely caused by the higher sorptivity of this mix (see Fig. 4).

383



384

385 **Fig. 6** Correlation between the percentage of cumulative mass loss and compressive strength
 386 loss at the end of 56 freeze-thaw cycles

387

388 **3.3.2 Flexural strength**

389

390 Table 7 summarises the average values of flexural strength, modulus of elasticity and toughness
 391 of the control and F-T specimens as obtained from testing three specimens per mix. Values in
 392 brackets represent standard deviation.

393

394 **Table 7** Average flexural strength, modulus of elasticity and toughness factor

| Mix | | 0P | 0BF | 30BF | 60BF |
|--------------------------------------|-----------------------|-----------|-----------|-----------|-----------|
| Flexural strength (MPa) | Control | 8.1 (1.1) | 9.4 (1.0) | 6.1 (1.0) | 3.7 (0.6) |
| | F-T | 8.5 (1.3) | 9.1 (0.5) | 4.9 (0.8) | 3.9 (0.6) |
| | Change on control (%) | 5 | -3 | -20 | 5 |
| Flexural modulus of elasticity (GPa) | Control | 48 (2.2) | 46 (0.1) | 26 (0.5) | 9.3 (1.0) |
| | F-T | 47 (4.3) | 44 (1.5) | 25 (0.7) | 8.8 (1.1) |
| | Change on control (%) | -3 | -3 | -3 | -5 |
| Flexural toughness factor (MPa) | Control | - | 5.9 (0.3) | 5.2 (0.9) | 3.2 (0.5) |
| | F-T | - | 5.2 (0.9) | 3.8 (0.7) | 3.4 (0.3) |
| | Change on control (%) | - | -12 | -27 | 6 |

395 Table 7 shows that the addition of blended fibres enhances the flexural strength of 0BF control
396 specimens by 5%, compared to 0P. On the other hand, the replacement of 30% and 60% of
397 natural aggregates with rubber particles, as expected, reduces the flexural strength by 35% and
398 60% respectively, compared to 0BF. It should be noted that the presence of steel fibres in
399 SFRRuC mixes effectively mitigates the rate of reduction in flexural strength, compared to that
400 in compressive strength, due to the ability of the fibres to control micro-cracking, as discussed
401 in Alsaif et al. [38].

402

403 After completing 56 cycles of freeze-thaw action, the concretes 0P, 0BF and 60BF show
404 comparable flexural strength values to those of control specimens of the same mixes with small
405 differences within one standard deviation. The flexural strength of the 30BF specimens after
406 56 cycles of freeze thaw action, however, is 20% below that of the control specimens of the
407 same mix, which is consistent with the reduction in compressive strength reported in Table 6.
408 As mentioned earlier, the high sorptivity in the 30BF mix [40] may have caused this reduction
409 in strength. Nevertheless, all SFRRuC specimens studied here (both F-T and control) satisfy
410 the flexural strength requirements specified in pavement design EN 13877-1[39].

411

412 3.3.3 Flexural modulus of elasticity

413

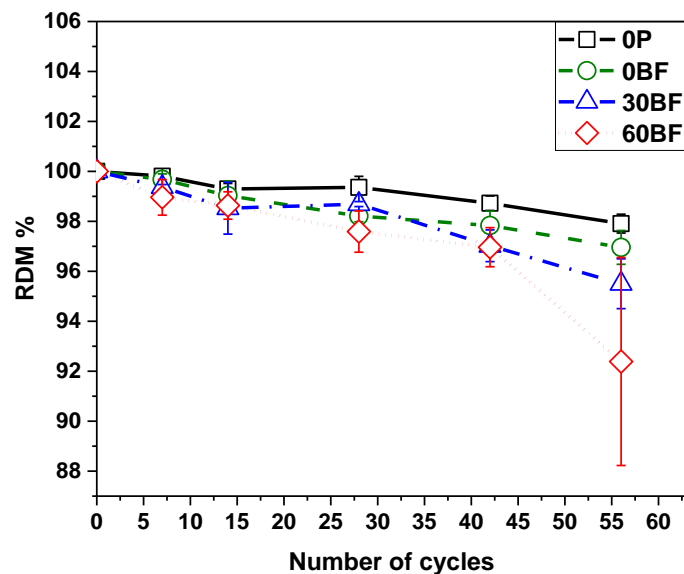
414 The elastic beam theory was adopted in this study to determine the secant modulus of elasticity
415 of the load-deflection curves considering the region from 0 to 40% of the peak load. As shown
416 in Table 7, the addition of steel fibres in conventional concrete specimens, 0BF, marginally
417 reduces the modulus of elasticity compared to 0P specimens. This reduction was not anticipated
418 as the addition of fibres was expected to slightly increase the modulus of elasticity of the
419 composite due to their high stiffness, but may be explained by the increased volume of
420 permeable voids, as discussed in [40]. The substantial decrease in the modulus of elasticity,
421 however, for the SFRRuC specimens (48% for 30BF and 80% for 60BF) was expected due to
422 the lower stiffness of the rubber aggregates, compared to the replaced natural aggregates [38].
423 After freeze-thaw action, minor reductions (3-5%) in the modulus of elasticity were recorded.
424 The RDM was also investigated and it is discussed in the following section.

425

3.3.3.1 Relative dynamic modulus of elasticity

427

428 Fig. 7 shows the mean RDM values as a function of the number of freeze-thaw cycles applied.
429 Error bars represent one standard deviation of three measurements. It is worth mentioning that,
430 during the periodical measurements, occasionally UPTT values went down due to difficulties
431 of making contact with the sides of the concrete prism as these were severely roughened due
432 to scaling. In general, the RDM values decrease with increasing number of freeze-thaw cycles.
433 This is expected due to the typical increase in water uptake (capillary pores imbibe water) and,
434 hence the UPTT values. It is also evident from Fig. 7 that the rate of reduction in RDM values
435 increases with the rubber content. This may indicate some loss in the bond between the rubber
436 and cementitious materials [1], possibly due to the weak adhesion in the interfacial transition
437 zone (ITZ). As all specimens survived 56 freeze-thaw cycles and their RDM values are above
438 the threshold value of 80% defined by RILEM 2004 [60], all concrete mixes can be considered
439 to be durable.



440

441 **Fig. 7** Change in relative dynamic modulus during freeze/thaw cycles

442

3.3.4 Load-deflection curve and flexural toughness factor

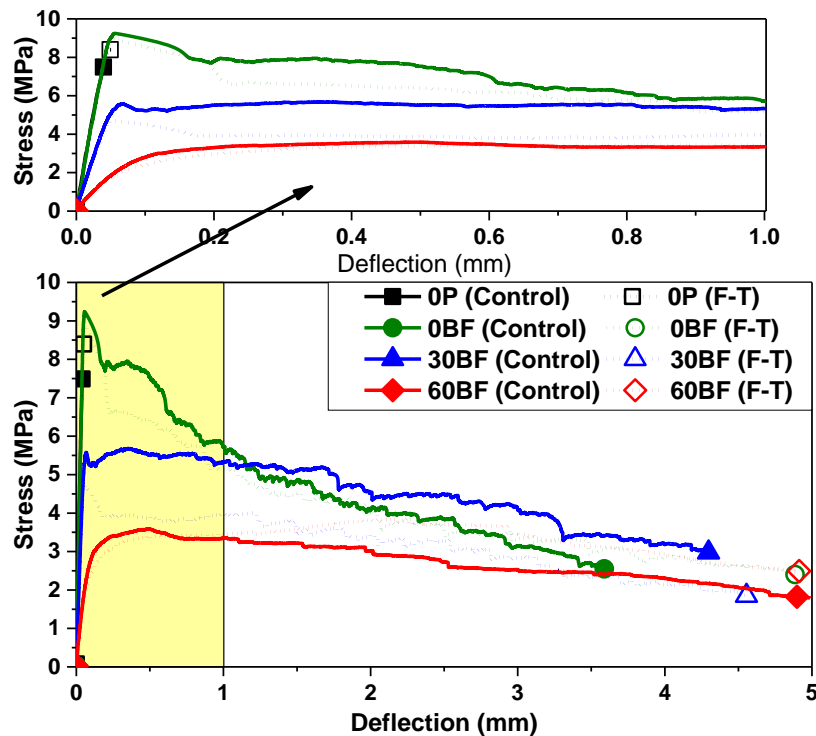
444

445 Fig. 8 shows the average (of 3 prisms) stress-deflection curves. While the plain concrete
446 specimens, OP, failed suddenly after reaching the peak stress, highlighting the brittleness of
447 plain concrete in tension, 0BF, 30BF and 60BF specimens continued sustaining further flexural
448 stresses even after first crack. This is mainly due to the contribution of fibres in dissipating

449 energy through their pull-out mechanism as well as in bridging cracks and resisting their
 450 opening [38]. Rubber particles also participated partially in enhancing the post-peak behaviour
 451 by absorbing some of the energy during loading and undergoing large deformation as identified
 452 by the authors in a previous study [38].

453

454



455

456 **Fig. 8** Average stress versus deflection curves for all concrete mixes

457

458 To further examine the effect of freeze-thaw action on the flexural behaviour of SFRC and
 459 SFRRuC, the flexural toughness factors were obtained (see Table 7) according to JSCE [51].
 460 The toughness factor of the plain concrete mix, 0P, is not included as its post-peak energy
 461 absorption behaviour is negligible. The area under the load-deflection curve is computed up to
 462 a deflection of $\delta_f = 2$ mm and the flexural toughness factor is calculated according to Equation
 463 (3).

464 Flexural toughness factor (MPa) =
$$\frac{\text{Area under the curve} \cdot L}{2 \cdot b \cdot h^2} \quad (3)$$

465 where L is the span length, in mm, b is the width of the specimen, in mm, h is the high of the
 466 specimen, in mm.

467 The toughness factor is found to decrease with increasing rubber content mainly due to the
468 large reduction in flexural strength. After freeze-thaw action, the toughness factor decreases by
469 12% for 0BF and 27% for 30BF while it increases by 6% for 60BF. Overall, F-T action did not
470 have a major impact on flexural performance, except for 30BF specimens due to their higher
471 sorptivity (see Fig. 4). This is mainly attributed to the presence of fibres which are more
472 effective in enhancing flexural behaviour through mechanisms (crack bridging) that are not
473 significantly affected by freeze-thaw.

474

475 **3.4 General discussion on practical use**

476

477 Previous research by the authors [38] showed that optimised flexible SFRRuC mixes were able
478 to attain high ductility and flexibility, and achieve workability properties and flexural strengths
479 that meet the specifications defined in pavement design [39]. It has also been identified in a
480 subsequent research study [40] that the durability and permeability properties of these flexible
481 SFRRuC mixes lie within the range of highly durable concrete based on commonly accepted
482 “durability indicators” [57, 60-62]. In this article, the authors demonstrate the ability of these
483 SFRRuC mixes to withstand 56 freeze-thaw cycles with acceptable scaling and without
484 presenting internal damage or degradation in mechanical performance. Furthermore, the
485 inclusion of a large amounts of waste tyre rubber leads to the development of flexible SFRRuC
486 pavements with stiffness values similar to those of flexible asphalt pavements, i.e. around 8
487 GPa [7]. Hence, these flexible SFRRuC are expected to accommodate subgrade induced
488 movements and settlements arising from poor compaction during construction or temperature
489 variations, including freeze-thaw. The body of this work shows that SFRRuC, which can be
490 manufactured using conventional mixing techniques, is a promising solution for building
491 sustainable road pavements.”

492

493 **4 Conclusion**

494

495 This study assessed the freeze-thaw performance of steel fibre reinforced rubberised concretes
496 (SFRRuC) produced with large contents of waste tyre rubber and reinforced with a blend of
497 manufactured and recycled tyre steel fibres. Based on the experimental results, this study shows
498 that all SFRRuC mixes successfully withstood 56 freeze-thaw cycles without being

499 significantly damaged. The cubes show acceptable scaling resistance according to the Swedish
500 Criteria SS 13 72 44 ED, while the prisms maintain RDMs values above the threshold value
501 for internal damage (80%) specified in RILEM TC 176-IDC. Hence, as hypothesised by the
502 authors, the inclusion of steel fibres in RuC greatly mitigates the negative effects of large
503 volumes of rubber on freeze-thaw resistance.

504

505 The presence of steel fibres in SFRRuC mixes significantly reduces the rate of reduction in
506 flexural strength due to the addition of large volumes of rubber, compared to that in
507 compressive strength. All SFRRuC mixes show flexural strengths that satisfy the requirement
508 for pavement design according to EN 13877-1.

509

510 Comparable mechanical performance is observed from specimens subjected to freeze-thaw and
511 control specimens kept in the mist room, thus making SFRRuC a potentially sustainable
512 flexible concrete pavement solution capable of adequate freeze-thaw performance. For
513 pavement applications, future studies should investigate the fatigue performance of this novel
514 concrete.

515

516 **Acknowledgements**

517

518 The current experimental work was undertaken under the FP7 European funded collaborative
519 project “Anagennisi: Innovative reuse of all tyre components in concrete” (Contract agreement
520 number: 603722). The following companies offered materials and valuable in-kind
521 contribution: Tarmac UK, Twincon Ltd, Aggregate Industries UK and Ltd Sika. Mr Alsaif
522 would like to thank King Saud University and the Ministry of Education (Kingdom of Saudi
523 Arabia) for sponsoring his PhD studies. Dr S.A. Bernal participation in this study has been
524 sponsored by EPSRC through her ECF (EP/R001642/1).

525

526

527

528 References

529

- 530 [1] K.A. Paine, R. Dhir, R. Moroney, and K. Kopasakis. *Use of crumb rubber to achieve freeze/thaw*
531 *resisting concrete*. in *Challenges of Concrete Construction: Volume 6, Concrete for Extreme*
532 *Conditions: Proceedings of the International Conference held at the University of Dundee,*
533 *Scotland, UK on 9–11 September 2002*. 2002: Thomas Telford Publishing.
- 534 [2] İ.B. Topçu and A. Demir. *Durability of rubberized mortar and concrete*. *Journal Of Materials In*
535 *Civil Engineering* 2007;19(2):173-178.
- 536 [3] A. Vaitkus, J. Gražulytė, E. Skrodenis, and I. Kravcovas. *Design of Frost Resistant Pavement*
537 *Structure Based on Road Weather Stations (RWSs) Data*. *Sustainability* 2016;8(12):1328.
- 538 [4] O.A. Abaza and Z.S. Hussein. *Flexural Behavior of Steel Fiber-Reinforced Rubberized Concrete*.
539 *Journal Of Materials In Civil Engineering* 2015;28(1):04015076.
- 540 [5] V. Baroghel-Bouny, P. Belin, M. Maultzsch, and D. Henry. *AgNO₃ spray tests: advantages,*
541 *weaknesses, and various applications to quantify chloride ingress into concrete. Part 1: Non-*
542 *steady-state diffusion tests and exposure to natural conditions*. *Materials and Structures*
543 2007;40(8):759-781.
- 544 [6] ETRA, *The European Tyre Recycling Association*. 2016, Available at: <http://www.etra-eu.org>
545 [Last accessed: 02/01/2018].
- 546 [7] Council of the European Union, *Council Directive 1999/31/EC of 26 April 1999 on the landfill*
547 *of waste*. 1999.
- 548 [8] N.N. Eldin and A.B. Senouci. *Measurement and prediction of the strength of rubberized*
549 *concrete*. *Cement and Concrete Composites* 1994;16(4):287-298.
- 550 [9] A. Benazzouk, O. Douzane, K. Mezreb, B. Laidoudi, and M. Queneudec. *Thermal conductivity*
551 *of cement composites containing rubber waste particles: Experimental study and modelling*.
552 *Construction and Building Materials* 2008;22(4):573-579.
- 553 [10] B.S. Mohammed, K.M.A. Hossain, J.T.E. Swee, G. Wong, and M. Abdullahi. *Properties of crumb*
554 *rubber hollow concrete block*. *Journal Of Cleaner Production* 2012;23(1):57-67.
- 555 [11] Council of the European Union, *Council Directive 2008/98/EC on waste (Waste Framework*
556 *Directive)*. 2008.
- 557 [12] J.A. Epps, *Uses of recycled rubber tires in highways*. Vol. 198. 1994: Transportation Research
558 Board.
- 559 [13] S.N. Amirkhanian and J.L. Burati Jr, *Utilization of waste tires in asphaltic materials*. *Clemson*
560 *Univ., SC (United States). Dept. of Civil Engineering. Technical Report;PB-96-203062/XAB,CNN:*
561 *Contract SPR-554; TRN: 62752193*. 1996.
- 562 [14] B. Adhikari, D. De, and S. Maiti. *Reclamation and recycling of waste rubber*. *Progress in*
563 *polymer science* 2000;25(7):909-948.
- 564 [15] S. Raffoul, R. Garcia, D. Escolano-Margarit, M. Guadagnini, I. Hajirasouliha, and K. Pilakoutas.
565 *Behaviour of unconfined and FRP-confined rubberised concrete in axial compression*.
566 *Construction and Building Materials* 2017;147:388-397.
- 567 [16] F. Hernández-Olivares and G. Barluenga. *Fire performance of recycled rubber-filled high-*
568 *strength concrete*. *Cement And Concrete Research* 2004;34(1):109-117.
- 569 [17] F. Hernández-Olivares, G. Barluenga, M. Bollati, and B. Witoszek. *Static and dynamic*
570 *behaviour of recycled tyre rubber-filled concrete*. *Cement And Concrete Research*
571 2002;32(10):1587-1596.
- 572 [18] A. Alsaif, R. Garcia, M. Guadagnini, and K. Pilakoutas, *Behaviour of FRP-Confined Rubberised*
573 *Concrete with Internal Recycled Tyre Steel Fibres*, in *High Tech Concrete: Where Technology*
574 *and Engineering Meet: Proceedings of the 2017 fib Symposium, held in Maastricht, The*
575 *Netherlands, June 12–14, 2017*, D.A. Hordijk and M. Luković, Editors. 2018, Springer
576 International Publishing: Cham. p. 233-241.
- 577 [19] A. Grinys, H. Sivilevičius, D. Pupeikis, and E. Ivanauskas. *Fracture of concrete containing crumb*
578 *rubber*. *Journal of Civil Engineering and Management* 2013;19(3):447-455.

- 579 [20] F. Liu, W. Zheng, L. Li, W. Feng, and G. Ning. *Mechanical and fatigue performance of rubber*
580 *concrete*. Construction and Building Materials 2013;47:711-719.
- 581 [21] S. Raffoul, R. Garcia, K. Pilakoutas, M. Guadagnini, and N.F. Medina. *Optimisation of*
582 *rubberised concrete with high rubber content: An experimental investigation*. Construction
583 and Building Materials 2016;124:391-404.
- 584 [22] P. Sukontasukkul and C. Chaikaew. *Properties of concrete pedestrian block mixed with crumb*
585 *rubber*. Construction and Building Materials 2006;20(7):450-457.
- 586 [23] T.C. Ling, H.M. Nor, and S.K. Lim. *Using recycled waste tyres in concrete paving blocks*.
587 Proceedings of the ICE - Waste and Resource Management 2010;163(1):37-45.
- 588 [24] C.A. Issa and G. Salem. *Utilization of recycled crumb rubber as fine aggregates in concrete mix*
589 *design*. Construction and Building Materials 2013;42:48-52.
- 590 [25] A.R. Khaloo, M. Dehestani, and P. Rahmatabadi. *Mechanical properties of concrete containing*
591 *a high volume of tire-rubber particles*. Waste management 2008;28(12):2472-2482.
- 592 [26] Z. Khatib and F. Bayomy. *Rubberized portland cement concrete*. Journal Of Materials In Civil
593 Engineering 1999;11(3):206-213.
- 594 [27] X. Zhu, C. Miao, J. Liu, and J. Hong. *Influence of crumb rubber on frost resistance of concrete*
595 *and effect mechanism*. Procedia Engineering 2012;27:206-213.
- 596 [28] A. Richardson, K. Coventry, V. Edmondson, and E. Dias. *Crumb rubber used in concrete to*
597 *provide freeze-thaw protection (optimal particle size)*. Journal Of Cleaner Production
598 2016;112:599-606.
- 599 [29] A.E. Richardson, K. Coventry, and G. Ward. *Freeze/thaw protection of concrete with optimum*
600 *rubber crumb content*. Journal Of Cleaner Production 2012;23(1):96-103.
- 601 [30] B. Savas, S. Ahmad, and D. Fedroff. *Freeze-thaw durability of concrete with ground waste tire*
602 *rubber*. Transportation Research Record: Journal of the Transportation Research Board
603 1997;(1574):80-88.
- 604 [31] ASTM, C666/C666M – 15: *Standard Test Method for Resistance of Concrete to Rapid Freezing*
605 *and Thawing*. 2015.
- 606 [32] A.J. Kardos and S.A. Durham. *Strength, durability, and environmental properties of concrete*
607 *utilizing recycled tire particles for pavement applications*. Construction and Building Materials
608 2015;98:832-845.
- 609 [33] T.C. Powers and T. Willis. *The air requirement of frost resistant concrete*. in *Highway Research*
610 *Board Proceedings*. 1950.
- 611 [34] T.C. Powers. *A working hypothesis for further studies of frost resistance of concrete*. in *Journal*
612 *Proceedings*. 1945.
- 613 [35] D.H. Bager. *Qualitative description of the micro ice body freeze-thaw damage mechanism in*
614 *concrete*. in *Workshop proceeding no. 9: Nordic miniseminar: Freeze-Thaw Testing of Concrete*
615 *– Input to revision of cen test methods*. 2010.
- 616 [36] B. Johannesson. *Dimensional and ice content changes of hardened concrete at different*
617 *freezing and thawing temperatures*. Cement and Concrete Composites 2010;32(1):73-83.
- 618 [37] A. Benazzouk, O. Douzane, T. Langlet, K. Mezreb, J. Roucoult, and M. Quéneudec. *Physico-*
619 *mechanical properties and water absorption of cement composite containing shredded rubber*
620 *wastes*. Cement and Concrete Composites 2007;29(10):732-740.
- 621 [38] A. Alsaif, L. Koutas, S.A. Bernal, M. Guadagnini, and K. Pilakoutas. *Mechanical performance of*
622 *steel fibre reinforced rubberised concrete for flexible concrete pavements*. Construction and
623 Building Materials 2018;172:533-543.
- 624 [39] BSI. *EN 13877-1. Concrete pavements Part 1: Materials*. BSI 389 Chiswick High Road London
625 W4 4AL UK. 2013.
- 626 [40] A. Alsaif, S.A. Bernal, M. Guadagnini, and K. Pilakoutas. *Durability of steel fibre reinforced*
627 *rubberised concrete exposed to chlorides*. Construction and Building Materials 2018;188:130-
628 142.
- 629 [41] ASTM, C136: *Standard test method for sieve analysis of fine and coarse aggregates*. ASTM
630 International, West Conshohocken, PA. doi:10.1520/C0136-06. 2006.

- 631 [42] H. Hu, P. Papastergiou, H. Angelakopoulos, M. Guadagnini, and K. Pilakoutas. *Mechanical*
632 *properties of SFRC using blended manufactured and recycled tyre steel fibres*. Construction
633 and Building Materials 2018;163:376-389.
- 634 [43] BSI, *BS 8500-1:2015+A1:2016. Concrete – Complementary British Standard to BS EN 206. Part*
635 *1: Method of specifying and guidance for the specifier*. 2016.
- 636 [44] BSI, *EN 12350-2: Testing fresh concrete, Part 2: Slump-test*. BSI 389 Chiswick High Road,
637 London W4 4AL, UK. 2009.
- 638 [45] BSI, *EN 12350-7: Testing fresh concrete, Part 7: Air content — Pressure*. BSI 389 Chiswick High
639 Road, London, W4 4AL, UK. 2009.
- 640 [46] BSI, *EN 12350-6: Testing fresh concrete Part 6: Density*. BSI 389 Chiswick High Road, London,
641 W4 4AL, UK. 2009.
- 642 [47] BSI, *EN 12390-2: Testing hardened concrete, Part 2: Making and curing specimens for strength*
643 *tests*. BSI 389 Chiswick High Road, London W4 4AL, UK. 2009.
- 644 [48] BSI, *PD CEN/TS 12390-9: Testing hardened concrete - Part 9: Freeze-thaw resistance with de-*
645 *icing salts - Scaling*. BSI 389 Chiswick High Road, London W4 4AL, UK. 2016.
- 646 [49] BSI, *PD CEN/TR15177: Testing the freeze-thaw resistance of concrete - Internal structural*
647 *damage*. BSI 389 Chiswick High Road, London W4 4AL, UK. 2006.
- 648 [50] BSI, *EN 12390-3: Testing hardened concrete, Part3: Compressive strength of test specimens*.
649 BSI 389 Chiswick High Road, London W4 4AL, UK. 2009.
- 650 [51] JSCE. *SF-4: Method of test for flexural strength and flexural toughness of steel fiber reinforced*
651 *concrete*. Japan Concrete Institute, Tokio, Japan. 1984.
- 652 [52] TI-B, 101. *Test Method. Expansion Coefficient of Concrete*. Danish Technological Institute
653 *Building Technology*. 1994.
- 654 [53] FDA, *Federal Highway Administration Research and Technology. Coordinating, Developing,*
655 *and Delivering Highway Transportation Innovations*. 2016.
- 656 [54] T. Harrison, J.D. Dewar, and B. Brown, *Freeze-thaw Resisting Concrete: Its Achievement in the*
657 *UK*. 2001: CIRIA.
- 658 [55] ASTM, *C672 / C672M-12: Standard Test Method for Scaling Resistance of Concrete Surfaces*
659 *Exposed to Deicing Chemicals*, ASTM International, West Conshohocken, PA, www.astm.org.
660 2012.
- 661 [56] J. Yuan, Y. Liu, H. Li, and C. Yang. *Experimental investigation of the variation of concrete pores*
662 *under the action of freeze-thaw cycles*. Procedia Engineering 2016;161:583-588.
- 663 [57] Swedish standards. *SS 13 72 44 ED. 4. Concrete Testing - Hardened Concrete - Scaling At*
664 *Freezing*. Standardiserings-Kommissionen I Sverige. 2005.
- 665 [58] G. Skripkiūnas, A. Grinys, and E. Janavičius. *Porosity and durability of rubberized concrete*. in
666 *The Second International Conference on Sustainable Construction Materials and Technologies*.
667 2010.
- 668 [59] K. Najim and M. Hall. *Mechanical and dynamic properties of self-compacting crumb rubber*
669 *modified concrete*. Construction and Building. Materials. 2012;27(1):521-530.
- 670 [60] RILEM, *TC 176-IDC: Internal damage of concrete due to frost action, Final Recommendation,*
671 *Prepared by L. Tang and P.-E. Petersson SP Swedish National Testing and Research Institute,*
672 *Boras, Sweden. Materials and Structures / Matériaux et Constructions, Vol. 37, December*
673 *2004, pp 754-759 in Slab test: Freeze/thaw resistance of concrete Internal deterioration 2004*.
- 674 [61] V. Baroghel-Bouny. *Evaluation and prediction of reinforced concrete durability by means of*
675 *durability indicators. Part I: new performance-based approach*. in *ConcreteLife'06-*
676 *International RILEM-JCI Seminar on Concrete Durability and Service Life Planning: Curing,*
677 *Crack Control, Performance in Harsh Environments*. 2006: RILEM Publications SARL.
- 678 [62] M. Alexander, J. Mackechnie, and Y. Ballim. *Guide to the use of durability indexes for achieving*
679 *durability in concrete structures*. Research monograph 1999;2.
- 680
- 681

